



---

Year: 2019

---

## Impact of high-speed sintering on translucency, phase content, grain sizes, and flexural strength of 3Y-TZP and 4Y-TZP zirconia materials

Jansen, Jan Ulrich ; Lümekemann, Nina ; Letz, Inge ; Pfefferle, Regina ; Sener, Beatrice ; Stawarczyk, Bogna

**Abstract:** STATEMENT OF PROBLEM: The lengthy sintering time of zirconia is costly and limits applications. The consequences of shortening the sintering time are mainly unknown. PURPOSE: The purpose of this in vitro study was to test and compare 2 high-speed sintering protocols and 1 conventional sintering protocol on the translucency, phase content, grain sizes, and flexural strength of 3 zirconia materials. MATERIAL AND METHODS: In total, 450 specimens of 3 zirconia materials-two were 3 mol% yttria-stabilized tetragonal zirconia polycrystals (3Y-TZPs), Ceramill ZI and Zolid (ZD), and a 4 mol% yttria-stabilized tetragonal zirconia polycrystal (4Y-TZP), Zolid HT+ (n=150)-and 5 thicknesses (1.0, 1.5, 2.0, 2.5, and 3.0 mm; n=30) were sintered according to 2 high-speed sintering protocols (final temperature 1570 °C and 1590 °C; n=10) and a reference sintering protocol (1450 °C; n=10). After measuring the monoclinic phase content with Raman spectrometry (n=3), the specimens were polished, and translucency was determined. The biaxial flexural strength of specimens with a thickness of 1.0 mm and 1.5 mm was tested (n=20). Statistical evaluation included 1-way ANOVA, the Kolmogorov-Smirnov, Kruskal-Wallis, Mann-Whitney-U, and Spearman-Rho tests and the Bonferroni correction (=0.0011). RESULTS: For ZI, the sintering protocols did not affect the translucency or biaxial flexural strength. ZD and HT+ showed significantly lower translucency for high-speed sintering protocols (P .001), but the biaxial flexural strength remained the same after the high-speed sintering protocol at 1590 °C. Grain sizes increased with increasing final sintering temperature for ZI and HT+, whereas translucency generally decreased with increasing material thickness. No monoclinic phase was detected in any group. CONCLUSIONS: The flexural strength was maintained with high-speed sintering but led to a decrease in translucency for ZD and HT+.

DOI: <https://doi.org/10.1016/j.prosdent.2019.02.005>

Posted at the Zurich Open Repository and Archive, University of Zurich

ZORA URL: <https://doi.org/10.5167/uzh-183101>

Journal Article

Accepted Version



The following work is licensed under a Creative Commons: Attribution-NonCommercial-NoDerivatives 4.0 International (CC BY-NC-ND 4.0) License.

Originally published at:

Jansen, Jan Ulrich; Lümke mann, Nina; Letz, Inge; Pfefferle, Regina; Sener, Beatrice; Stawarczyk, Bogna (2019). Impact of high-speed sintering on translucency, phase content, grain sizes, and flexural strength of 3Y-TZP and 4Y-TZP zirconia materials. *Journal of Prosthetic Dentistry*, 122(4):396-403.  
DOI: <https://doi.org/10.1016/j.prosdent.2019.02.005>

JPD-18-475

## RESEARCH AND EDUCATION

Impact of high-speed sintering on translucency, phase content, grain sizes, and flexural strength of 3Y-TZP and 4Y-TZP zirconia materials

Jan Ulrich Jansen, BSc<sup>a</sup>, Nina Lümke, MSc<sup>b</sup>, Inge Letz, DDT<sup>c</sup>, Regina Pfefferle, BSc<sup>d</sup>, Beatrice Sener, MTA<sup>e</sup>, PD Dr. Dipl. Ing. (FH) Bogna Stawarczyk, MSc<sup>f</sup>

<sup>a</sup> Research Associate of Dental Material Unit, Department of Prosthetic Dentistry, Dental School, Ludwig-Maximilians-University Munich, Germany.

<sup>b</sup> Research Associate of Dental Material Unit, Department of Prosthetic Dentistry, Dental School, Ludwig-Maximilians-University Munich, Germany.

<sup>c</sup> Dental Technician, Department of Prosthetic Dentistry, Material Science, Dental School, Ludwig-Maximilians-Universität, Munich, Germany.

<sup>d</sup> Research Associate of Dental Material Unit, Department of Prosthetic Dentistry, Dental School, Ludwig-Maximilians-University Munich, Germany.

<sup>e</sup> Medical Technologist Assistant, Clinic for preventive dentistry, periodontics and cardiology, University of Zurich, Switzerland.

<sup>f</sup> Scientific Head of Dental Material Unit, Department of Prosthetic Dentistry, Dental School, Ludwig-Maximilians-University Munich, Germany.

Corresponding author:

PD Dr. Dipl. Ing. (FH) Bogna Stawarczyk, MSc  
Department of Prosthetic Dentistry

Dental School, Ludwig-Maximilians-Universität München

Goethestrasse 70, 80336 Munich GERMANY

Email: bogna.stawarczyk@med.uni-muenchen.de

## ABSTRACT

**Statement of problem.** The lengthy sintering time of zirconia is costly and limits applications.

The consequences of shortening the sintering time are mainly unknown.

**Purpose.** The purpose of this in vitro study was to test and compare 2 high-speed sintering protocols and 1 conventional sintering protocol on the translucency, phase content, grain sizes, and flexural strength of 3 zirconia materials.

**Material and methods.** In total, 450 specimens of 3 zirconia materials, two were 3 mol% yttria-stabilized tetragonal zirconia polycrystals (3Y-TZP): Ceramill ZI and Zolid (ZD) and a 4 mol% yttria-stabilized tetragonal zirconia polycrystal (4Y-TZP) Zolid HT+ (n=150) and 5 thicknesses (1.0, 1.5, 2.0, 2.5, and 3.0 mm; n=30) were sintered according to 2 high-speed sintering protocols (final temperature 1570 °C and 1590 °C; n=10) and a reference sintering protocol (1450 °C; n=10). After measuring the monoclinic phase content with Raman spectrometry (n=3), the specimens were polished, and translucency was determined. The biaxial flexural strength of specimens with a thickness of 1.0 mm and 1.5 mm, was tested (n=20). Statistical evaluation included 1-way ANOVA, the Kolmogorov-Smirnov, Kruskal-Wallis, Mann-Whitney-U, and Spearman-Rho tests and the Bonferroni correction ( $\alpha=.0011$ ).

**Results.** For ZI, the sintering protocols did not affect translucency or biaxial flexural strength. ZD and HT+ showed significantly lower translucency for high-speed sintering protocols ( $P\leq.001$ ), but the biaxial flexural strength remained after the high-speed sintering protocol at

1590 °C. Grain sizes increased with increasing final sintering temperature for ZI and HT+, while translucency generally decreased with increasing material thickness. No monoclinic phase was detected in any group.

**Conclusions.** The flexural strength was maintained with high-speed sintering but led to a decrease in translucency for ZD and HT+.

## CLINICAL IMPLICATION

Shorter zirconia sintering times are attractive because of reduced treatment time, fewer treatment appointments, and lower cost. Dentists should be aware of the relevant effects of high-speed sintering on the mechanical, morphological, and optical properties of the different formulations of zirconia materials.

## INTRODUCTION

The advantages of zirconia, such as biocompatibility, esthetics, and high strength, make it a popular material for dental restorations.<sup>1</sup> Furthermore, wear of the opposing dentition does not appear to be a problem if the restoration is properly finished.<sup>2</sup> However, the long sintering time of up to 12 hours, which is used to establish the final structure and properties of the material, lengthens the patient's treatment and restricts its use for direct applications. Another challenge is the difficulty in combining high translucency with high mechanical properties.<sup>3</sup> The flexural strength and translucency of the various zirconias with different amounts of yttria ( $Y_2O_3$ ) and alumina ( $Al_2O_3$ ) are compared in Table 1. For this study, tetragonal (contrast ratio (CR): 0.74<sup>4</sup>,  $\sigma$ : 1215 MPa<sup>4</sup>), tetragonal with reduced  $Al_2O_3$  (CR: 0.69<sup>4</sup>,  $\sigma$ : 983 MPa<sup>4</sup>) 3 mol% yttria-stabilized tetragonal zirconia polycrystal (3Y-TZP), and as the tetragonal and cubic third 5 mol% yttria-

stabilized tetragonal zirconia polycrystal (5Y-TZP) (CR: 0.65<sup>4</sup>,  $\sigma$ : 539 MPa<sup>4</sup>) were evaluated (Table 2).<sup>3-6</sup> However, since 5Y-TZP does not fulfill the mechanical requirements for multiple-unit fixed dental prostheses (FDPs),<sup>6</sup> 4 mol% yttria-stabilized tetragonal zirconia polycrystal (4Y-TZP) was developed to represent a compromise between 3Y-TZP with reduced Al<sub>2</sub>O<sub>3</sub> and 5Y-TZP (Table 1).

When shorter sintering time is considered, such as 60 to 120 minutes (speed-sintering) and 10 minutes (high-speed sintering), at least a constant translucency for (high-) speed compared with conventional sintering has been reported for tetragonal zirconia.<sup>7,8</sup> Such high-speed sintering protocols (10 minutes, 1580 °C) lead to higher flexural strength than conventional sintering.<sup>9</sup> The short sintering duration of 10 minutes can be realized by preheating the furnace, although there are furnaces that can produce sintering times of 30 minutes without preheating for direct applications. Technologies such as electromagnetic induction heating or inductively coupled plasma have been used to minimize overloading the heater elements because of higher temperatures and higher heating rates as well as to enhance the heat transfer.<sup>10</sup> In order to maintain the energy input for a short sintering time, the final sintering temperature has been increased, reducing the strength of the first developed 3Y-TZP at sintering times of 120 minutes from 1600 °C upwards.<sup>11</sup> Grain size and translucency increases have been reported with increasing sintering temperatures.<sup>11-15</sup> However, decreases in translucency with shorter sintering times have been reported together with increased grain size.<sup>8</sup>

The translucency of zirconia depends on scattering, reflection, absorption, and transmission. For Y<sub>2</sub>O<sub>3</sub>-stabilized zirconia, adsorption has been reported not to influence the translucency significantly.<sup>16</sup> Transmission and reflection occur according to the refraction at interfaces, which is influenced by pores, impurities, defects, and grain boundaries,<sup>16</sup> and the

material's refractive index. The additive  $\text{Al}_2\text{O}_3$  is said to assist the sintering but reduces the translucency, since the  $\text{Al}_2\text{O}_3$  grains are smaller and more segregated near the grain boundaries of zirconia.<sup>17-21</sup> At the same time,  $\text{Al}_2\text{O}_3$  limits the grain growth and affects diffusion.<sup>18,20,22</sup> Furthermore, birefringence, which takes place for tetragonal but not for cubic zirconia, leads to refractive index changes at grain boundaries and explains why there are fewer scattering effects and higher translucency for zirconia in the cubic phase<sup>16</sup>: this relates to the 4Y-TZP and the 5Y-TZP. Translucency and flexural strength are influenced by the microstructure of the material. Translucency decreases with an increase in the number of grain boundaries and thus correlates with the grain size of the material and the material thickness.<sup>11</sup> Vacancies and inclusions lower translucency because of additional scattering and refraction and reduce flexural strength because of less bonding between grains. Smaller grains increase the flexural strength.<sup>16,19,23-25</sup>

Raman spectrometry is a suitable method for analyzing the monoclinic phase content of zirconia,<sup>26-28</sup> because it can differentiate the monoclinic ( $178\text{ cm}^{-1}$ ) and tetragonal ( $190\text{ cm}^{-1}$ ) phases, has high depth resolution, can be applied to unprepared surfaces, and thus is nondestructive.<sup>29</sup>

The null hypotheses of this in vitro study were that specimen thickness would not affect translucency and that the tested high-speed sintering protocols, the choice of zirconia generation, and the combination of factors would not affect the translucency, monocline phase content, grain size, or flexural strength of 3Y-TZP with 0.05 and 0.25 wt%  $\text{Al}_2\text{O}_3$  and 4Y-TZP.

## **MATERIAL AND METHODS**

As listed in Table 2, 15-mm-diameter disks of the two 3Y-TZPs (ZI, ZD) and the 4Y-TZP (HT+) were selected for the tests and processed according to 3 sintering protocols (Fig. 1). In total, 450

specimens (n=150 per zirconia material) were milled (Ceramill motion 2; Amann Girrbach AG), ground (SiC abrasive paper P1200; Buehler), and sintered (high-speed sintered groups: self-optimized furnace, reference groups: Therm 2; Amann Girrbach AG) with n=50 per sintering protocol. High-speed sintering protocols were characterized by a final temperature of 1570 °C or 1590 °C and a holding time of 10 minutes. The third sintering protocol with the final temperature of 1450 °C and a holding time of 120 minutes functioned as a control.

Raman spectrometry (InVia Qontor; Renishaw) (n=3 per subgroups) was used to analyze monoclinic phase content. Nine hundred spectra were captured in the center of the specimens with the help of 2-dimensional-mapping technology (streamHR WiRE 4.4, build 6602; Renishaw). This was realized with a step size of 1.00  $\mu\text{m}^{-1}$  on an area of 30×30  $\mu\text{m}$ , a spectral range from 57.46  $\text{cm}^{-1}$  to 1839.07  $\text{cm}^{-1}$ , a laser wavelength of 523 nm, an acquisition time of 1 second, and a diffraction grating of 1800 lines/mm. The measurement time per specimen was 18 minutes.

For the translucency investigations, specimen thicknesses of 1.0, 1.5, 2.0, 2.5, and 3.0 mm (n=10 per subgroup) were evaluated. Nine specimens of the same thickness were simultaneously polished (Abramin; Struers) with diamond pads (40  $\mu\text{m}$  and 20  $\mu\text{m}$ ), grinding pads (9  $\mu\text{m}$  and 3  $\mu\text{m}$ ), and a polishing pad (1  $\mu\text{m}$ ) in combination with diamond suspensions (Struers). Translucency was measured with a UV/Vis spectrophotometer (Lambda 35; PerkinElmer). The specimens were cleaned (Alkopharm 80; Brüggemann Alcohol Heilbronn), mounted with modeling clay (BLU TACK; Bostik) and positioned at the inlet hole of the integrating sphere. The measurements were made at room temperature (23 °C) in a dry and darkened environment. The spectrometer continuously recorded the light transmission coefficients for the range from 400 nm to 700 nm at 2-nm intervals and generated the absolute



results by comparison with source values via split beam optics (transmitted intensity/source intensity). The percentile translucency was calculated by integrating this fraction over the wavelength from 400 nm to 700 nm and referencing it to the integrated value with no specimen (baseline).

Grain sizes (n=1 per subgroup) were determined with scanning electron microscopy (Carl Zeiss Supra 50VP FESEM, Carl Zeiss) (SEM) with an acceleration voltage of 5.0 kV at a working distance of 7.5 mm. Before analysis, thermal etching (30 minutes by 1450 °C; LTH 02/16; Nabertherm) was performed as well as sputtering (Sputter Coater Safematic CCU-010; Safematic) with tungsten in a 2-nm- thick layer. The surface was recorded at 3 different areas per specimen and analyzed with regard to pores, grain size, blowholes, and impurities.

For biaxial flexural strength determination (n=20 per subgroup), 1-mm and 1.5-mm specimens were tested with a 5.1-mm-radius bearing ball, an 0.8-mm-radius piston, and a crosshead speed of 1 mm/min at room temperature (23 °C) (Zwick/Roell Z 2.5; Zwick). The flexural strength was calculated by the following formula:

$$\sigma = -0.2387 P (X - Y)/d^2,$$

where  $\sigma$ =flexural strength (MPa),  $P$ =fracture load (N),  $d$ =specimen thickness (mm), and the coefficients  $X$  and  $Y$ :

$$X = (1 + \nu)\ln (r_2/r_3)^2 + [(1 - \nu)/(r_2/r_3)^2]$$

$$Y = (1 + \nu)[1 + \ln (r_1/r_3)^2] + (1 - \nu)(r_1/r_3)^2,$$

where  $\nu$ =Poisson ratio,  $r_1$ =bearing ball radius (mm),  $r_2$ = piston radius (mm),  $r_3$ =specimen radius (mm).

Global univariate ANOVA with additional partial eta-squared ( $\eta_p^2$ ) determination was performed to evaluate the influences of the 3 factors (zirconia material, sintering protocol, and

thickness) on the flexural strength and translucency results. This indicated whether a further evaluation should be performed in subgroups or in pooled data records. Statistical evaluation of the results was performed beginning with a descriptive analysis followed by the Kolmogorov-Smirnov to test the violation of the normal distribution. The Kruskal-Wallis and Mann-Whitney-U tests were conducted to analyze significant differences between the tested groups.

Two-way ANOVA with the post hoc Scheffé and  $\eta_p^2$  was calculated to analyze the effect of the material and sintering protocol on the size of the grains. The Spearman-Rho test was used to calculate the correlation between the specimen thicknesses and translucency values for each test group separately (IBM SPSS Statistics, v23; IBM Corp).  $\alpha$  was adjusted by using a Bonferroni correction ( $0.05/45=.0011$ ).

## RESULTS

The Raman spectra evaluation did not detect monoclinic phase content for any group and thus no effect of either the material thickness, the choice of zirconia, or the sintering protocol (Fig. 2).

The biggest influence on the translucency was exerted by the specimen thickness (partial eta squared  $\eta_p^2=.972$ ,  $P<.001$ ), followed by the sintering protocol ( $\eta_p^2=.905$ ,  $P<.001$ ) and the choice of zirconia ( $\eta_p^2=.486$ ,  $P<.001$ ). The effect of the binary or ternary combinations of the 3 parameters was significant only for the combination of zirconia material and sintering protocol ( $\eta_p^2=.760$ ,  $P<.001$ ). Therefore, the results were analyzed separately according to the tested hypotheses. Concerning translucency, the Kolmogorov-Smirnov test indicated a violation of normality assumption regarding the distribution of the data for 18% of all tested groups.

As shown in Figure 3, the translucency values decreased with increasing specimen thickness ( $P<.001$ , Spearman-Rho correlation: -0.970 to -0.980), except between 1 mm and

1.5 mm of the group ZD reference sintered at 1450 °C ( $P=.002$ ). The highest translucency values were observed for ZD with 1 mm thickness and all thicknesses of HT+ sintered using the reference sintering. The lowest translucency values were measured for ZI specimens sintered at 1570 °C with 1-mm thickness and for ZD specimens sintered at 1590 °C with thicknesses from 1.5 mm to 3 mm. In specimens sintered using reference sintering, HT+ resulted in higher translucency than ZD, and ZD was higher than ZI ( $P<.001$ ). Except in 1-mm specimens, ZD and HT+ were in the same value range ( $P=.940$ ). In 1570 °C high-speed sintered specimens with thicknesses from 2 mm to 3 mm, ZI and HT+ showed higher translucency than ZD ( $P<.001$ ). In 1-mm-thick specimens, ZD was more translucent than ZI ( $P<.001$ ). In 1.5-mm specimens, ZD resulted in higher translucency than ZD ( $P<.001$ ). In 1590 °C sintered specimens, no differences were observed in 1-mm thick specimens ( $P\geq.650$ ). For 1.5-mm-thick specimens, ZI and HT+ showed higher translucency values than ZD ( $P<.001$ ). In specimens of thicknesses between 2 mm and 3 mm, ZI presented the highest translucency values, followed by HT+ and ZD ( $P\leq.001$ ). Reference sintering resulted in higher translucency than high-speed sintering for ZD and HT+ for all thicknesses and for ZI with thicknesses between 2.5 mm and 3 mm ( $P<.001$ ). Both high-speed sintered groups were in the same value range ( $P\geq.131$ ).

The results of the SEM recordings are shown in Table 3. The surfaces showed similar microstructure, and grain sizes were perceptibly different. However, SEMs of ZI at both high-speed sintering revealed undulating textures of the grains. The grouped values were normally distributed. The sintering protocol ( $\eta_p^2=.538$ ,  $P<.001$ ) showed the highest impact on the grain sizes, followed by the material ( $\eta_p^2=.306$ ,  $P=.001$ ). High-speed sintering at 1590 °C revealed the highest grain sizes followed by high-speed sintering at 1570 °C, while the reference sintering showed the smallest grain sizes. Among the materials, ZI resulted in the highest grain sizes,

while HT+ and ZD were comparable. No interactions were found between sintering protocol and material ( $P=.635$ ). Sintering protocol did not show significant differences between the grain sizes for HT+, although for ZI and ZD, differences occurred ( $P<.001$ ). Reference sintering resulted in the smallest grain sizes followed by high-speed sintering at 1570 °C and 1590 °C. The analysis of the material choice revealed no significant differences for the sintering protocols with a final temperature of 1450 °C and 1590 °C. For 1570 °C, ZI showed coarser grains ( $0.22 \mu\text{m}^2$ ) than ZD ( $0.17 \mu\text{m}^2$ ) ( $P=.042$ ). The morphological observations (Fig. 4) illustrate more homogenous grain sizes and finer grains for 3Y-TZP both after reference sintering and the high-speed sintering protocols.

For the flexural strength data, the highest impact was for choice of zirconia ( $\eta_p^2=.150$ ,  $P<.001$ ), followed by sintering protocol ( $\eta_p^2=.085$ ,  $P=.001$ ). The material thickness ( $P\geq.218$ ) did not affect the biaxial flexural strength results. As a result, further statistical investigations were performed with thickness pooled data. A fraction of 22% of the groups was not normally distributed. The choice of material did not affect the strength outcomes of the high-speed sintering protocol at 1590 °C (Table 3). With reference and 1570 °C sintering, ZI showed significantly higher biaxial flexural strength values than ZD ( $P\leq.001$ ). The value for HT+ was located between those of ZI and ZD. For ZI, the sintering protocol did not affect the biaxial flexural strength ( $P\geq.536$ ). HT+ showed the same behavior ( $P\geq.006$ ). ZD showed higher biaxial flexural strength for high-speed sintering at 1590 °C than at 1570 °C ( $P\leq.001$ ) (Fig. 5).

## DISCUSSION

The compatibility of shorter sintering time, clinically sufficient strength, translucency, and stable microstructure without defects was the focus of this study. The stated null hypotheses were

rejected except that regarding the monoclinic phase content, which was confirmed. An inversely proportional correlation of material thickness and translucency (Fig. 3) was found for all groups. This correlation is consistent with the findings of previous investigations and can be ascribed to Lambert's law, which describes the logarithmic relationship of intensity attenuation of radiation.<sup>4,24</sup> However, the results were not tested for the logarithmic relationship or its variables.

An increase in translucency from ZI, followed by ZD and HT+ was observed, presumably because of their chemical composition and the resulting altered microstructure. The sintering additive  $\text{Al}_2\text{O}_3$  and the stabilizer  $\text{Y}_2\text{O}_3$  influenced the grain size and phase content, thus effecting birefringence and the translucency of the zirconia.<sup>4,16,19</sup> When high-speed sintering is conducted, the ZD and HT+ zirconias with less  $\text{Al}_2\text{O}_3$  had significantly lower translucency (Table 2). The high-speed sintering protocols used high sintering temperatures and short sintering times. Increased density of particles in the pressed blank, reduction of pore spaces, [phase transformation](#), and formation or growth of grains during sintering all explain how the shortened sintering time or the fast temperature rates may cause lower translucency.<sup>16</sup> For 3Y-TZP with reduced  $\text{Al}_2\text{O}_3$  (ZD) diffusion or repositioning processes take place, which leads to the location of  $\text{Al}_2\text{O}_3$  at the grain boundaries, which results in lower translucency.<sup>19</sup> When  $\text{Al}_2\text{O}_3$  is located evenly in the crystal lattice, it increases the birefringence because it has a different refractive coefficient to zirconia, which may explain the lower translucency after high-speed sintering. A different response to high-speed sintering appears to exist among the zirconia materials, and ZD and HT+ require precautions when sintered at high temperatures or at short sintering times. However, the earlier 3Y-TZP (ZI) becomes more translucent with higher sintering temperatures<sup>11</sup> and is not affected by the sintering protocol.

SEM images were made of the unpolished state to determine the reasons for differences in translucency and grain sizes. These demonstrated that the influence of the final temperature outweighs the grain growth because of the longer sintering duration. Grains became coarser with higher final sintering temperatures (Fig. 4). Furthermore, the images confirm the larger grain size for 3Y-TZP with 0.25 wt% than with 0.05 wt%  $\text{Al}_2\text{O}_3$  (Fig. 4). According to the SEM images (Fig. 4), translucency differences due to pores, inclusions, or other phenomena at grain level can be excluded for the high-speed sintering protocols.

Although, a larger grain size has been reported to compromise strength,<sup>16</sup> the results of the present study suggest that reasons other than grain size must predominate. Additionally, the degree of sintering does not explain the findings, since the high-speed sintering protocol at 1590 °C had higher mean flexural strength than that of the control sintering protocol ( $P \leq .001$ ). Surprisingly, HT+ resulted in comparable flexural strength values with the other 2 materials ( $P = .101$ ), while ZD and ZI were significantly different ( $P \leq .001$ ). For the high-speed sintering protocol at 1590 °C, ZD resulted in significantly coarser grains ( $P \leq .001$ ) and higher strength ( $P \leq .001$ ), which indicated that the higher temperature affected the mechanical properties.

The absence of measurable monoclinic phase content in any group supports the theory that the different behavior caused by the sintering protocol was not influenced by changes in the crystal lattice but by macroscopic factors including grain sizes, diffusion processes, and densification, which could not be assessed by the Raman spectrometry analysis. A limitation of this study was the lack of power analysis to determine sample size, it is not clear if the sample size was adequate. Further studies with equal testing arrangements, parameters, and evaluation techniques should be conducted to allow the comparison of research results. Information derived from geometrical specimens need to be verified in anatomical

reconstructions simulating the clinical situation. Of course, clinical studies are also needed to support the use of high-speed sintered zirconia FDPs for long-term restorations.

## **CONCLUSIONS**

Within the limitations of this in vitro study, the following conclusions were drawn:

1. 3Y-TZP with 0.05 wt%  $\text{Al}_2\text{O}_3$  resulted in a higher biaxial flexural strength for high-speed sintering at 1590 °C than at 1570 °C.
2. The translucency of 3Y-TZP with 0.05 wt%  $\text{Al}_2\text{O}_3$  and 4Y-TZP was reduced when high-speed sintering was compared with the control groups.

## REFERENCES

1. Alfawaz Y. Zirconia crown as single unit tooth restoration: A literature review. *J Contemp Dent Pract* 2016;17:418-22.
2. Kwon SJ, Lawson NC, McLaren EE, Nejat AH, Burgess JO. Comparison of the mechanical properties of translucent zirconia and lithium disilicate. *J Prosthet Dent* 2018;120:132-7.
3. Stawarczyk B, Keul C, Eichberger M, Figge D, Edelhoff D, Lumkemann N. Three generations of zirconia: From veneered to monolithic. Part II. *Quintessence Int* 2017;48:441-50.
4. Carrabba M, Keeling AJ, Aziz A, Vichi A, Fabian Fonzar R, Wood D et al. Translucent zirconia in the ceramic scenario for monolithic restorations: A flexural strength and translucency comparison test. *J Dent* 2017;60:70-6.
5. Vichi A, Sedda M, Fabian Fonzar R, Carrabba M, Ferrari M. Comparison of contrast ratio, translucency parameter, and flexural strength of traditional and "Augmented Translucency" zirconia for CEREC CAD/CAM System. *J Esthet Restor Dent* 2016;28 Suppl 1:S32-9.
6. Nassary Zadeh P, Lumkemann N, Sener B, Eichberger M, Stawarczyk B. Flexural strength, fracture toughness, and translucency of cubic/tetragonal zirconia materials. *J Prosthet Dent* 2018;120:948-54.
7. Kaizer MR, Gierthmuehlen PC, Dos Santos MB, Cava SS, Zhang Y. Speed sintering translucent zirconia for chairside one-visit dental restorations: Optical, mechanical, and wear characteristics. *Ceram Int* 2017;43:10999-1005.
8. Kim MJ, Ahn JS, Kim JH, Kim HY, Kim WC. Effects of the sintering conditions of dental zirconia ceramics on the grain size and translucency. *J Adv Prosthodont* 2013;5:161-6.



9. Ersoy NM, Aydogdu HM, Degirmenci BU, Cokuk N, Sevimay M. The effects of sintering temperature and duration on the flexural strength and grain size of zirconia. *Acta Biomater Odontol Scand* 2015;1:43-50.
10. Carden RA, Maginnis S, Paskalov G, Szeremeta A, inventors. James R. Glidewell Dental Ceramics, Inc., assignee. Method of rapid sintering of ceramics. WO/2012/057829; 2012.
11. Stawarczyk B, Ozcan M, Hallmann L, Ender A, Mehl A, Hammerlet CH. The effect of zirconia sintering temperature on flexural strength, grain size, and contrast ratio. *Clin Oral Investig* 2013;17:269-74.
12. Inokoshi M, Zhang F, De Munck J, Minakuchi S, Naert I, Vleugels J et al. Influence of sintering conditions on low-temperature degradation of dental zirconia. *Dent Mater* 2014;30:669-78.
13. Jiang L, Liao Y, Wan Q, Li W. Effects of sintering temperature and particle size on the translucency of zirconium dioxide dental ceramic. *J Mater Sci Mater Med* 2011;22:2429-35.
14. Zhang F, Inokoshi M, Batuk M, Hadermann J, Naert I, Van Meerbeek B et al. Strength, toughness and aging stability of highly-translucent Y-TZP ceramics for dental restorations. *Dent Mater* 2016;32:e327-e37.
15. Ebeid K, Wille S, Hamdy A, Salah T, El-Etreby A, Kern M. Effect of changes in sintering parameters on monolithic translucent zirconia. *Dent Mater* 2014;30:e419-24.
16. Zhang Y. Making yttria-stabilized tetragonal zirconia translucent. *Dent Mater* 2014;30:1195-203.
17. Zhang H, Li Z, Kim B-N, Morita K, Yoshida H, Hiraga K, et al. Effect of alumina dopant on transparency of tetragonal zirconia. *J Nanomater* 2012;2012:1-5.

18. Suzuki TS, Sakka Y, Morita K, Hiraga K. Enhanced superplasticity in a alumina containing zirconia prepared by colloidal processing. *Scr Mater* 2000;43:705-10.
19. Stawarczyk B, Keul C, Eichberger M, Figge D, Edelhoff D, Lumkemann N. Three generations of zirconia: From veneered to monolithic. Part I. *Quintessence Int* 2017;48:369-80.
20. Macan J, Brcković L, Gajović A. Influence of preparation method and alumina content on crystallization and morphology of porous yttria stabilized zirconia. *J Eur Ceram Soc* 2017;37:3137-49.
21. Ross IM, Rainforth WM, McComb DW, Scott AJ, Brydson R. The role of trace additions of alumina to yttria-tetragonal zirconia polycrystals (Y-TZP). *Scr Mater* 2001;45:653-60.
22. Yu Q, Zhou C, Zhang H, Zhao F. Thermal stability of nanostructured 13 wt%  $\text{Al}_2\text{O}_3$ –8 wt%  $\text{Y}_2\text{O}_3$ – $\text{ZrO}_2$  thermal barrier coatings. *J Eur Ceram Soc* 2010;30:889-97.
23. Kim HK, Kim SH, Lee JB, Han JS, Yeo IS, Ha SR. Effect of the amount of thickness reduction on color and translucency of dental monolithic zirconia ceramics. *J Adv Prosthodont* 2016;8:37-42.
24. Abdelbary O, Wahsh M, Sherif A, Salah T. Effect of accelerated aging on translucency of monolithic zirconia. *Future Dental Journal* 2016;2:65-9.
25. Wang F, Takahashi H, Iwasaki N. Translucency of dental ceramics with different thicknesses. *J Prosthet Dent* 2013;110:14-20.
26. Wulfman C, Djaker N, Sadoun M, Lamy de la Chapelle M, Clarke D. 3Y-TZP In-depth phase transformation by Raman spectroscopy: A comparison of three methods. *J Am Ceram Soc* 2014;97:2233-40.

27. Inokoshi M, Zhang F, Vanmeensel K, De Munck J, Minakuchi S, Naert I, et al. Residual compressive surface stress increases the bending strength of dental zirconia. *Dent Mater* 2017;33:e147-e54.
28. Belli R, Wendler M, Zorzin JI, Lohbauer U. Practical and theoretical considerations on the fracture toughness testing of dental restorative materials. *Dent Mater* 2018;34:97-119.
29. Wulfman C, Sadoun M, Lamy de la Chapelle M. Interest of Raman spectroscopy for the study of dental material: The zirconia material example. *Irbm* 2010;31:257-62.
30. DIN EN ISO 6872:2015 Dentistry -- Ceramic materials. Berlin 2015.  
<https://www.iso.org/standard/59936.html>.

## TABLES

Table 1. Zirconia. Translucency and flexural strength

Zirconia	Translucency (%)	Biaxial Flexural Strength (MPa)
3Y-TZP	20 <sup>3</sup>	1200 <sup>3</sup>
3Y-TZP (reduced Al <sub>2</sub> O <sub>3</sub> )	25 <sup>3</sup>	1000 <sup>3</sup>
5Y-TZP	35 - 40 <sup>3</sup>	500 <sup>3</sup>
4Y-TZP	30	900
Desirable values for single unit FDP (lateral tooth area)	N/A	100 <sup>30</sup>
Desirable values for multiple-unit FDP	N/A	800 <sup>30</sup>

Table 2. Materials. Abbreviation and composition (\* not tested in study)

Zirconia	Materials	Abbreviation	Y <sub>2</sub> O <sub>3</sub> content [mol%]	Al <sub>2</sub> O <sub>3</sub> content [wt%]	LOT
3Y-TZP	Ceramill ZI	ZI	3	0.25	5306033B 5306496B 1710001
3Y-TZP (reduced Al <sub>2</sub> O <sub>3</sub> )	Ceramill Zolid	ZD	3	0.05	ZY306361B 306043B 1710000
5Y-TZP	Ceramill Zolid FX	N/A	5	0.05	N/A*
4Y-TZP	Ceramill Zolid HT+	HT+	4	0.05	170303 XY406356G

Table 3. Biaxial flexural strength and grain sizes (Asterisks indicate groups that deviate from normal deviation. Lowercase letters indicate significant impact due to choice of sintering protocol in separated groups. Uppercase letters indicate significant impact of material respectively. Same superscript letters indicate no significant difference between values.) HT+, Ceramill Zolid HT+; SEM, scanning electron microscopy; ZD, Ceramill Zolid ; ZI, Ceramill ZI

Material	Sintering Protocol (°C)	Grain size Mean $\pm$ SD ( $\mu\text{m}^2$ )	Biaxial Flexural Strength Min / Median / Max (MPa)
ZI	1570	0.22 $\pm$ 0.02 <sup>bB</sup>	1084 / 1251 / 1435 <sup>aB</sup>
	1590	0.26 $\pm$ 0.01 <sup>cA</sup>	993 / 1241 / 1414 <sup>aA</sup>
	1450	0.17 $\pm$ 0.01 <sup>aA</sup>	1001 / 1251 / 1571 <sup>aB</sup>
ZD	1570	0.17 $\pm$ 0.01 <sup>bA</sup>	827 / 1023 / 1214 <sup>*aA</sup>
	1590	0.21 $\pm$ 0.03 <sup>cA</sup>	872 / 1220 / 1480 <sup>bA</sup>
	1450	0.13 $\pm$ 0.01 <sup>aA</sup>	892 / 1080 / 1273 <sup>abA</sup>
HT+	1570	0.19 $\pm$ 0.05 <sup>aAB</sup>	677 / 1146 / 1287 <sup>aAB</sup>
	1590	0.20 $\pm$ 0.07 <sup>aA</sup>	1059 / 1257 / 1398 <sup>aA</sup>
	1450	0.14 $\pm$ 0.04 <sup>aA</sup>	347 / 1126 / 1445 <sup>*aAB</sup>

## FIGURES

Figure 1. Study design. HT+, Ceramill Zolid HT+; SEM, scanning electron microscopy; ZD, Ceramill Zolid; ZI, Ceramill ZI.

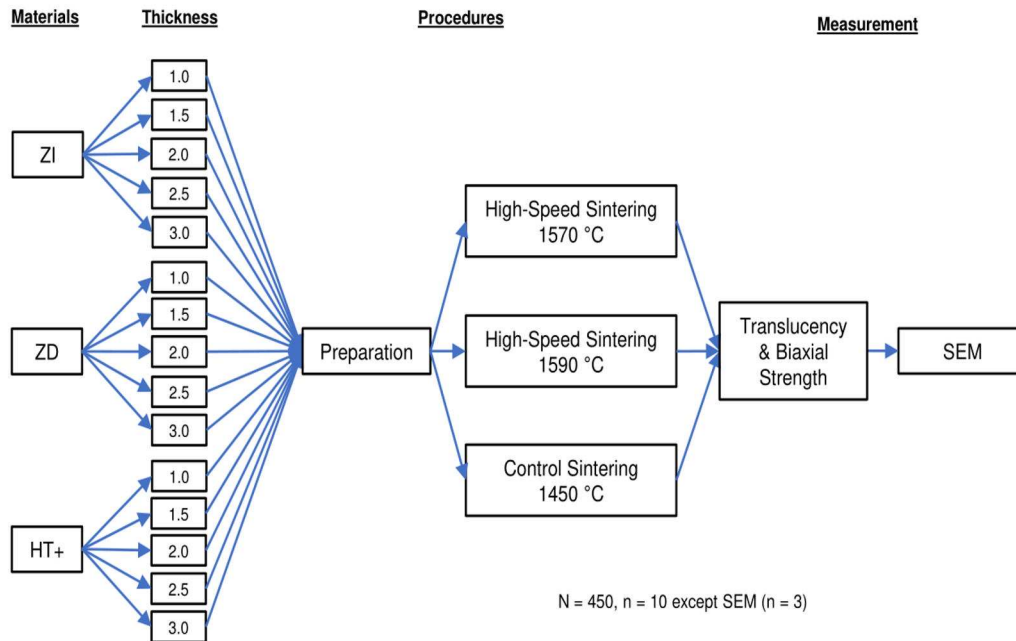


Figure 2. Raman spectra of Ceramill ZI sintered at final temperature of 1570 °C and thickness of 1 mm.

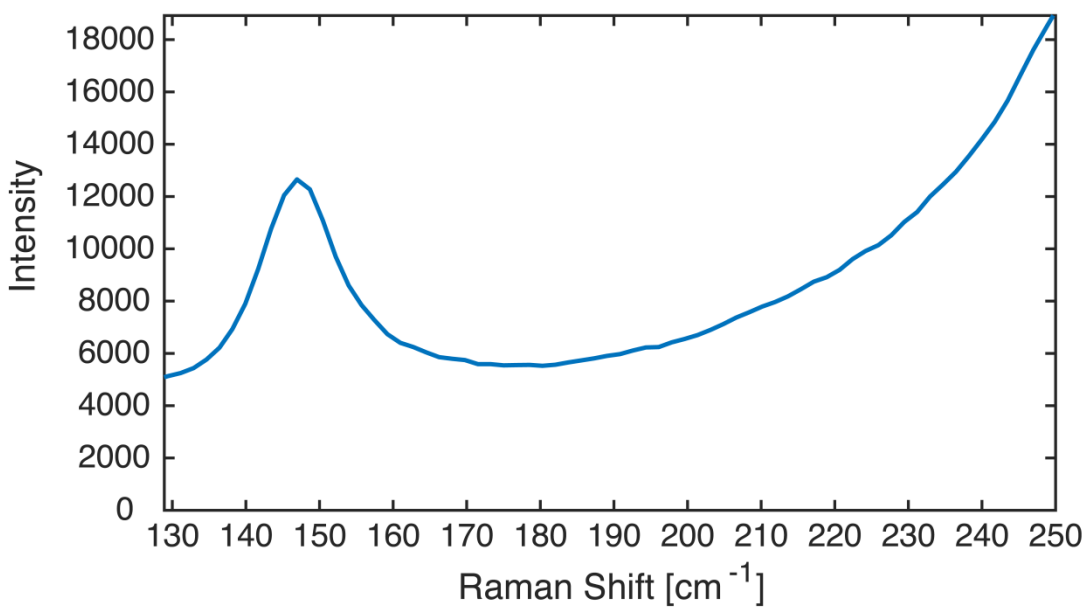


Figure 3. Translucency grouped by material and sintering protocol. (Impact of specimen thicknesses is significantly different ( $P \leq .001$ ), except between 1 mm and 1.5 mm of group ZD at 1450 °C. ° and \* indicate outliers and strong outliers).

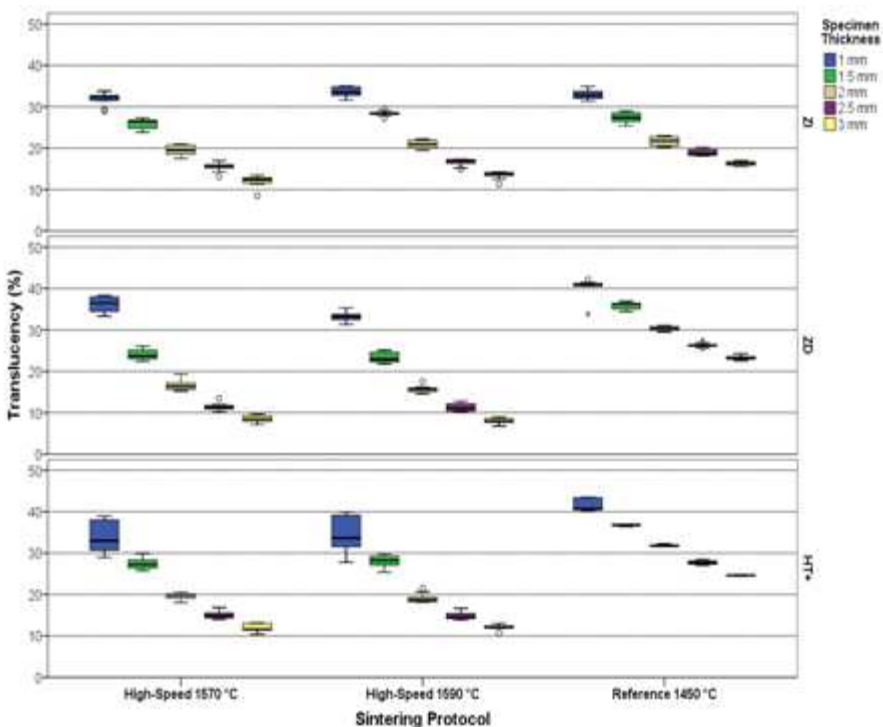




Figure 4. Scanning electron microscope images [showing](#) impact of sintering protocol and material on grain size and morphology. Original magnification  $\times 50\,000$ . HT+, Ceramill Zolid HT+; ZD, Ceramill Zolid; ZI, Ceramill ZI.

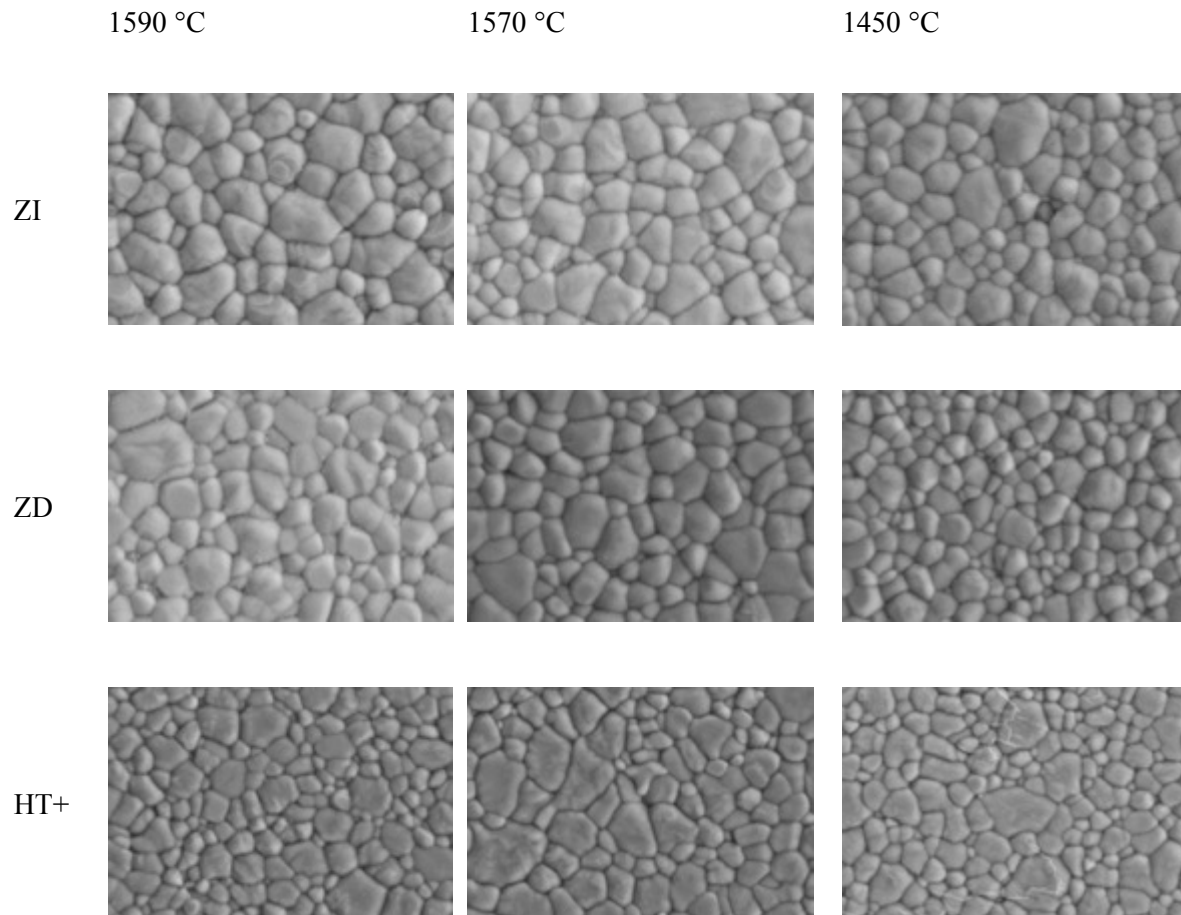


Figure 5. Flexural strength grouped by material and sintering protocol. (° and \* indicate outliers and strong outliers). HT+, Ceramill Zolid HT+; ZD, Ceramill Zolid; ZI, Ceramill ZI.

